

12

A136288

FINAL REPORT

Reattachment of a Three-Dimensional,
Incompressible Jet to an Adjacent
Axisymmetric Inclined Surface

March 31, 1983

Grant No. AFOSR-82-0215

Principal Investigator:

Eugene E. Niemi, Jr.
University of Lowell
Lowell, Massachusetts 01854

DTIC
ELECTRONIC
S DEC 27 1983
A

DTIC FILE COPY

Approved for public release;
Distribution unlimited.

83 12 27 16

REPORT DOCUMENTATION PAGE		READ INSTRUCTIONS BEFORE COMPLETING FORM
1. REPORT NUMBER AFOSR-TR-83-1225	2. GOVT ACCESSION NO.	3. RECIPIENT'S CATALOG NUMBER
4. TITLE (and Subtitle) REATTACHMENT OF A THREE-DIMENSIONAL, INCOMPRESSIBLE JET TO AN ADJACENT AXISYMMETRIC INCLINED SURFACE		5. TYPE OF REPORT & PERIOD COVERED FINAL 15 Apr 82 - 31 Jan 83
		6. PERFORMING ORG. REPORT NUMBER
7. AUTHOR(s) EUGENE E NIEMI JR		8. CONTRACT OR GRANT NUMBER(s) AFOSR-82-0215
9. PERFORMING ORGANIZATION NAME AND ADDRESS UNIVERSITY OF LOWELL RESEARCH FOUNDATION 450 AIKEN STREET LOWELL, MA 01854		10. PROGRAM ELEMENT, PROJECT, TASK AREA & WORK UNIT NUMBERS 61102F 2307/D9
11. CONTROLLING OFFICE NAME AND ADDRESS AIR FORCE OFFICE OF SCIENTIFIC RESEARCH/NA BOLLING AFB, DC 20332		12. REPORT DATE March 1983
		13. NUMBER OF PAGES 44
14. MONITORING AGENCY NAME & ADDRESS (if different from Controlling Office)		15. SECURITY CLASS. (of this report, UNCLASSIFIED
		15a. DECLASSIFICATION/DOWNGRADING SCHEDULE
16. DISTRIBUTION STATEMENT (of this Report) Approved for Public Release; Distribution Unlimited.		
17. DISTRIBUTION STATEMENT (of the abstract entered in Block 20, if different from Report)		
18. SUPPLEMENTARY NOTES		
19. KEY WORDS (Continue on reverse side if necessary and identify by block number) THRUST REVERSER COANDA EFFECT REATTACHMENT THREE-DIMENSIONAL FLOW		
20. ABSTRACT (Continue on reverse side if necessary and identify by block number) A study has been made of the fluid mechanics of a thrust reverser jet reattaching to an aircraft nozzle afterbody. The problem basically involves the Coanda effect flow of a three-dimensional, incompressible jet to an adjacent axisymmetric, inclined surface. The equations have been derived in integral form and programmed for numerical solution for the case of an exhaust flow with no opposing free stream flow. Test data are reported for a scale model of a nozzle afterbody exhausting against a target-type thrust reverser. Data are presented for surface pressure coefficient at various		

UNCLASSIFIED

SECURITY CLASSIFICATION OF THIS PAGE(When Data Entered)

points along the model. Recommendations are made for future research in this area.

CLASSIFIED

SECURITY CLASSIFICATION OF THIS PAGE(When Data Entered)

Abstract

↪ A study ^{was} ~~has~~ been made of the fluid mechanics of a thrust reverser jet reattaching to an aircraft nozzle afterbody. The problem basically involves the Coanda effect flow of a three-dimensional, incompressible jet to an adjacent axisymmetric, inclined surface.

The equations ^{were} ~~have~~ been derived in integral form and programmed for numerical solution for the case of an exhaust flow with no opposing free stream flow.

Test data are reported for a scale model of a nozzle afterbody exhausting against a target-type thrust reverser. Data are presented for surface pressure coefficient at various points along the model.

Recommendations are made for future research in this area.



For	
<input checked="checked" type="checkbox"/>	
<input type="checkbox"/>	
<input type="checkbox"/>	
Distribution/	
Availability Codes	
Avail and/or	
Dist	Special
A-1	

AIR FORCE OFFICE OF SCIENTIFIC RESEARCH (AFOSR)
NOTICE OF TRANSMITTAL TO DTIC
This technical report has been reviewed and is
approved for public release in accordance with AFM 100-12.
Distribution is unlimited.
MATTHEW J. KEMPER
Chief, Technical Information Division

Table of Contents

	<u>Page</u>
I. Introduction and Background	1
II. Literature Survey	1
III. Development of Theory	3
Assumptions and Equations	4
Solution of Equations	8
IV. Experimental Work	9
Test Results.	12
V. Solution of Flow Equations.	13
VI. Recommendations for Future Work	15
VII. Conclusions	16
References.	17
Nomenclature.	19
Appendix A, Computer Program Printout	A-1
Appendix B, Summary of Test Data.	B-1

I. Introduction and Background

The U.S. Air Force has shown recent interest in the use of thrust reversers on future models of fighter aircraft. Thrust reversers are being considered for use both as a tactical maneuvering device in the transonic speed range, as well as for more conventional use during the landing mode.

A number of problems can arise when thrust reversers are used on aircraft. One particular problem that can occur when thrust reversers are deployed in flight is the attachment of the reversed jet to the aircraft afterbody and fuselage. This phenomenon has been reported in wind tunnel tests of full size aircraft in references 1 and 2, and for model scale wind tunnel tests in reference 3.

The current research is for the purpose of developing a theoretical method for predicting conditions under which a reversed exhaust jet will attach to an aircraft afterbody. The original proposal for this research is reference 4.

II. Literature Survey

The thrust reverser flow attachment is basically a variation of the Coanda effect. The Coanda effect finds one of its more useful applications in the field of fluidics. Therefore, some of the work reviewed is related to fluidics.

One of the earliest analyses of Coanda effect that was studied in detail was the work of Bourque and Newman⁵. Bourque and Newman developed a simplified theory for predicting jet attachment distance for a two-dimensional, incompressible jet exiting near an adjacent flat plate. In this study, the surrounding fluid was at rest.

Experimental data were also reported and compared with the theory. The agreement was generally fair to good.

Bourque and Newman described the jet attachment hysteresis effect in terms of the range of angles over which an incompressible jet would attach to an adjacent sidewall. It was found that the flow could be attached or detached depending on how the flow was initiated.

Perry⁶ developed a theory for predicting reattachment location for an incompressible jet by making several improvements to the theory of reference 5. Perry compared his theory with his own experimental data as well as the experimental data of reference 5, and it was shown that some improvement was obtained in the agreement between theory and experiment.

Olson⁷ extended the above studies to two dimensional, compressible flow, and compared the theory to test data. Olson's theory involved a trial and error numerical procedure. Two values of constants that appear in the theory had to be evaluated from experimental data. The theory was developed to handle both setback and slope of side walls.

In reference 8, an experimental study was made of the effect of jet Reynolds number on location of attachment point. It was found that a hysteresis effect occurred for flow attachment in terms of an upper and lower Reynolds number. Experiments and flow visualization were done for low speed water flows. The experiments were done for a three-dimensional, rectangular exit nozzle geometry roughly approximating two-dimensional conditions. No theory was developed in this reference.

The most recent work located on this topic was that of Hoch and Jiji⁹. They extend the theory of references 5 and 6 and develop a theoretical model to predict incompressible jet reattachment in the presence of a parallel free stream. More realistic assumptions are made for pressure, velocity, and jet radius of curvature in the preattachment region. The model uses boundary layer type velocity profiles and a semi-empirical pressure spread coefficient determined from comparisons with experimental data. Good correlation is obtained between theory and experimental data.

A study of a thrust reverser's effect on the exhaust jet flow field was performed by Sarpkaya and Hiriart¹⁰. A detailed study was made of the effect of various thrust reverser shapes on the shape and orientation of the flow leaving the reverser. However, no work was done on subsequent reattachment of the jet to the aircraft afterbody.

It is seen that no work appears to have been done on the problem of the reattachment of an axisymmetric jet to an aircraft afterbody.

III. Development of Theory

A number of possible theoretical approaches are possible -- the one to be taken based on time and funds available for the conduct of the project. Various potential flow and perfect fluid theories are available, a number of these available in computer code form, such as finite difference and finite element analyses. These might be useful in determining the pressure and velocity field in the neighborhood of the jet, but cannot be used to determine the jet behavior itself (such as attachment conditions), because the attachment effect is a viscous entrainment phenomenon.

Ordinary viscous flow theories, such as boundary layer programs, will probably not be directly useful either, since they do not allow for the type of fluid entrainment and flow against a primary main stream that is occurring in this problem.

Considerable time was spent reviewing different theoretical approaches that might be applied to the problem, including the advanced methods presented in references 11 and 12. Based on this review, it was decided that the time and funds available would have to limit the study to the development of a basic theory to predict the essential characteristics of the flow being studied. As will be seen in later sections, some of the inputs to the theory required obtaining some experimental data, and a slight shift in the emphasis originally proposed.

Assumptions and Equations

The approach used for this investigation is illustrated in Figure 1. The flow from the nozzle afterbody exits rearward in the +Z

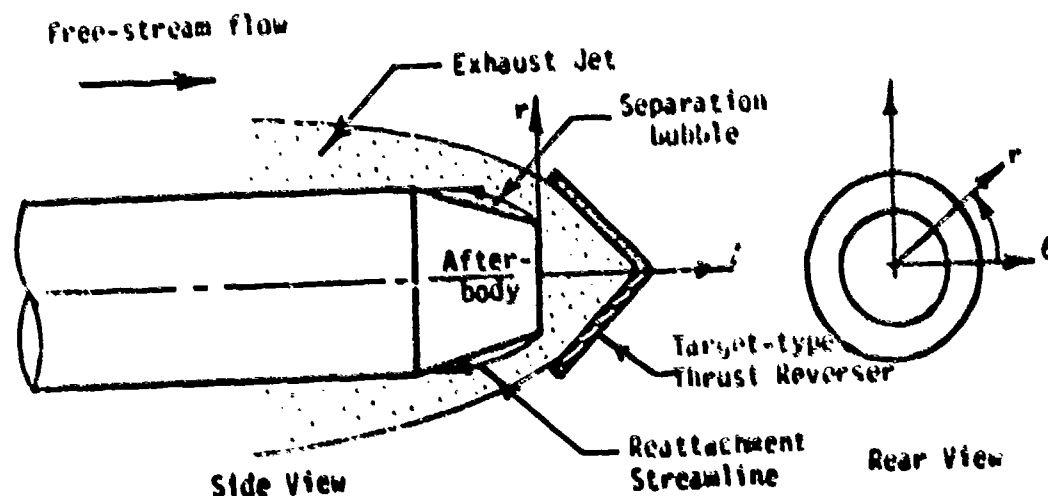


Figure 1. Flow Geometry for Reattached Jet

direction until it hits the target-type thrust reverser, whereupon the flow is turned forward in a direction generally parallel to the sloping afterbody sides. For the case of flow reattachment, a separation bubble is formed between the jet exit and the point where the flow finally reattaches to the afterbody. The geometry of the nozzle/afterbody was chosen similar to one of those investigated experimentally for other effects in reference 13.

The assumptions that have been made to develop the theory are as follows:

- 1) Steady, incompressible flow.
- 2) Three dimensional, axisymmetric flow.
- 3) Exhaust flow is Newtonian fluid.
- 4) Negligible diffusion between flows.
- 5) Entrainment of fluid similar to that of a free jet.

This leads to an integral approach to the problem, with simplified models for the entrainment effects and pressure and velocity profiles.

The geometry used for derivation of the equations for the flow field is shown in Figure 2.

The derivation generally follows the approach presented in reference 7, but with modifications as necessary to account for differences in geometry. Semi-empirical factors for the theory might also be different and have to be obtained from experiments. All symbols are defined in the nomenclature section of this report.

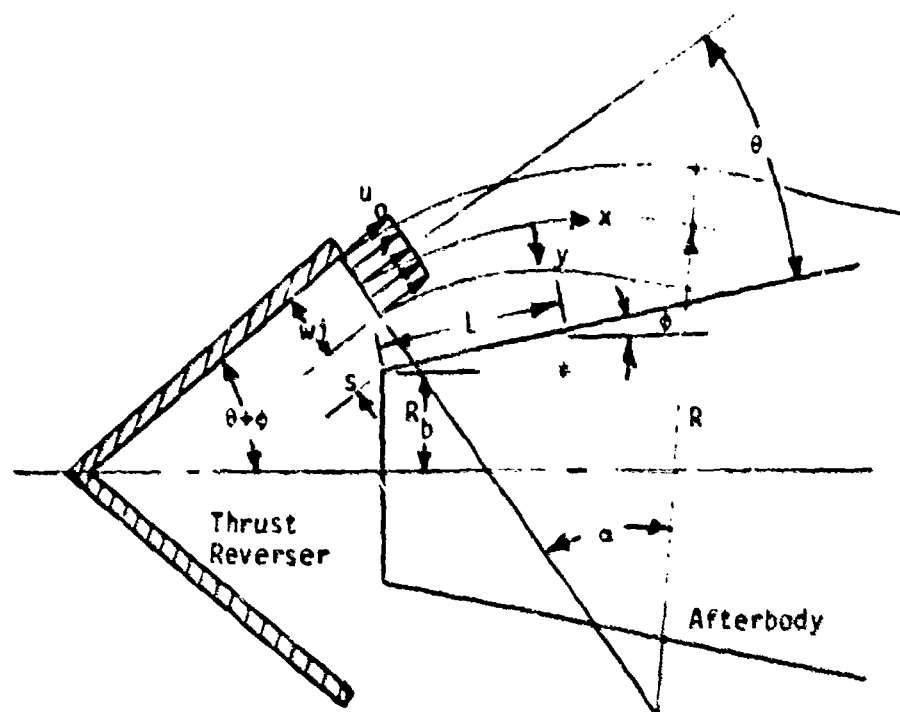


Figure 2. Flow Field Near Reattachment

The radius of curvature of the exhaust jet is given by

$$R = \left[\frac{(\rho u_0^2 / \rho_0) R_j w_j}{1 - p_1 / p_0} \right]^{1/2} \quad (1)$$

The non-dimensional distance between the jet centerline and the boundary wall, Δ/w_j is given by

$$\frac{\Delta}{w_j} = \frac{R}{w_j} - \left\{ \left(\frac{L}{w_j} \cos \theta \right)^2 + \left[\frac{R}{w_j} - \left(\frac{1}{2} + \frac{S}{w_j} + \frac{L}{w_j} \sin \theta \right) \right]^2 \right\}^{1/2} \quad (2)$$

The non-dimensional distance along the jet centerline is given by

$$\frac{x}{w_j} = \frac{R}{w_j} \alpha \quad (3)$$

where the angle α is given by

$$\alpha = \tan^{-1} \left[\frac{\frac{L}{w_j} \cos \theta}{\frac{R}{w_j} - \left(\frac{L}{w_j} \sin \theta + \frac{s}{w_j} + \frac{1}{2} \right)} \right] \quad (4)$$

The velocity distribution in the jet is assumed to satisfy the equation⁵

$$u = \left[\frac{3 J \alpha}{4 \rho (x + x_0)} \right]^{1/2} \operatorname{sech}^2 \frac{\sigma y}{x + x_0} \quad (5)$$

The position of the separation streamline, δ/w_j , is obtained by numerically integrating the mass flow in the jet from the centerline for small increases in y/w_j , assuming the jet characteristics upstream of reattachment are given by (5). The integration is continued until the mass flow equals one-half the mass flow in the jet at the point where it leaves the thrust reverser. The resulting value of y/w_j is taken as the position of the separation streamline.

With δ/w_j known, equations (1) through (4) can be used to calculate the reattachment location as a function of the mean pressure in the separation bubble using the condition that $\Delta/w_j = \delta/w_j$ at reattachment.

The mean pressure in the separation bubble, divided by the pressure on the free boundary of the jet becomes

$$\frac{p_1}{p_e} = 1 + \left(\frac{I_0 + I_1}{A p_0} \right) \cos \alpha - K_2 \left(\frac{p_s}{p_0} - 1 \right) \frac{A' \cos \alpha}{A} - \frac{\rho_0 U_0^2}{p_0} \left(\frac{2\pi R/w_j}{A} \right) \quad (6)$$

In this equation, I_0 is the momentum of all the flow in the downstream direction at x'/w_j , and I_1 is the momentum of the downstream flow at x'/w_j that is reversed back into the separation bubble at reattachment. The stagnation pressure on the separation streamline is given by p_s , and K_2 is an empirical constant related to the fraction of

pressure force effective in reversing the flow momentum at reattachment.

The area expressions in equation (6) are given in equations (7) and (8):

$$A = 2\pi R' (s + L' \sin \theta) + \pi (s + L' \sin \theta)^2 \cos (\theta + \phi) \quad (7)$$

$$A' = 2\pi R' (\Delta' - \delta') + \pi (\Delta' - \delta')^2 \cos [\alpha - (\theta + \phi)] \quad (8)$$

In equation (7), L' is the value of L to the point in the jet where the static pressure can be assumed constant across the jet and equal to the static pressure on the outer boundary of the jet. The location of this downstream boundary at x'/w_j is taken as some fraction K_1 of the value of x/w_j at reattachment. The value of K_1 must be determined empirically.

Solution of Equations

Equations (1) through (8) can be solved by an iteration technique similar to that proposed in reference (7) to determine the jet reattachment location for the case where there is a reattaching exhaust jet flow but no opposing free stream flow. The equations also give the jet trajectory in the preattachment region, the axial velocity decay in the jet, and the wall pressure in the separation bubble. The case of free stream flow is discussed in Section VI.

In order to solve these equations, however, two empirical constants, K_1 and K_2 are needed, as well as use of an empirical jet spread equation. Evaluation of the existing literature has revealed no available jet spread equation for axisymmetric flow that can be

used as a more accurate replacement for equation (5). This equation predicts the effects of both jet spread and entrainment for a two dimensional jet.

To validate any solutions from the theory outlined above, some experimental data will eventually be needed. Thus, it became apparent that some change in the emphasis of the original research proposal would be necessary, a change from a completely theoretical study to a theoretical study supplemented by experiments. As a result, a parallel experimental study was undertaken and is described in the next section. Some results of the theory are discussed in Section V.

IV. Experimental Work

Figure 3 is an illustration of a model that has been constructed to study flow reattachment in three-dimensional axisymmetric flow. The nozzle-afterbody section of the model is similar in design to one used in tests reported in reference 13.

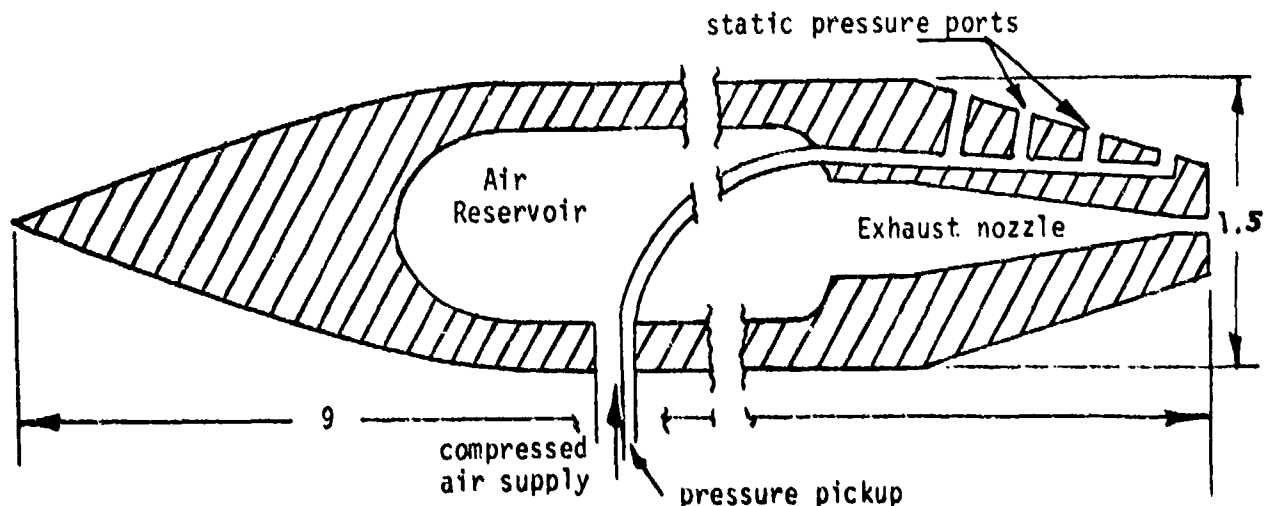


Figure 3. Schematic of Model Used for Experiments

The model is provided with compressed air which discharges through a conventional aft-mounted nozzle. Not shown in the figure is a target-type thrust reverser which causes the exhaust to flow forward along the afterbody. Four static pressure orifices located along the afterbody were used to measure pressures.

Figures 4a and 4b are photographs of the model and its mounting for the University of Lowell low speed wind tunnel. Tests were conducted at several free-stream velocities and nozzle pressure ratios, and at various thrust reverser set-back distances. Two sizes of nozzle throat opening were tested.

A matrix of the more important conditions tested is given in Table 1. Tests were made at other conditions also, but are not reported in this study.

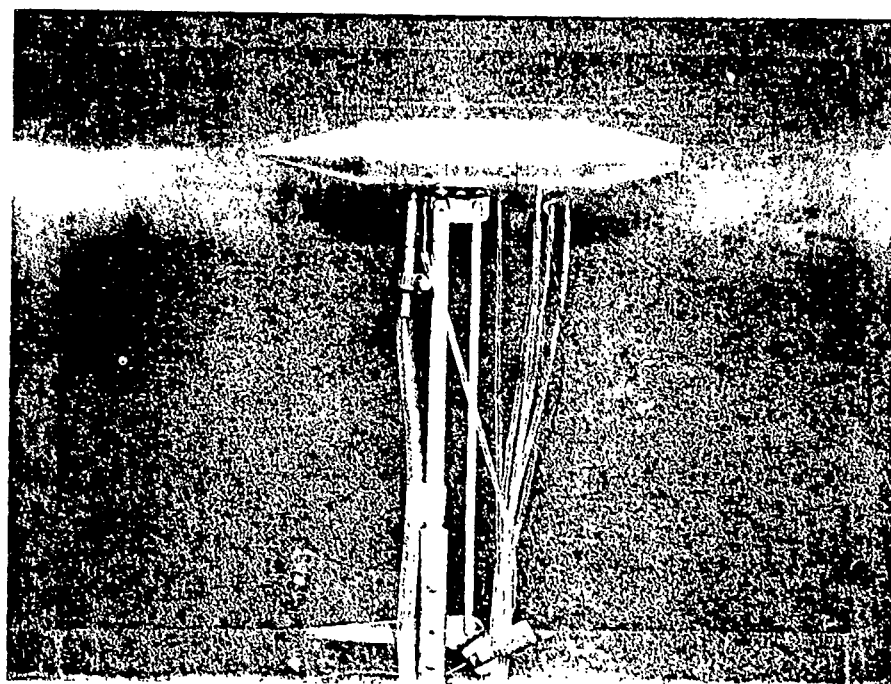


Figure 4a. Model Showing Pressure Pickups
and Compressed Air Line

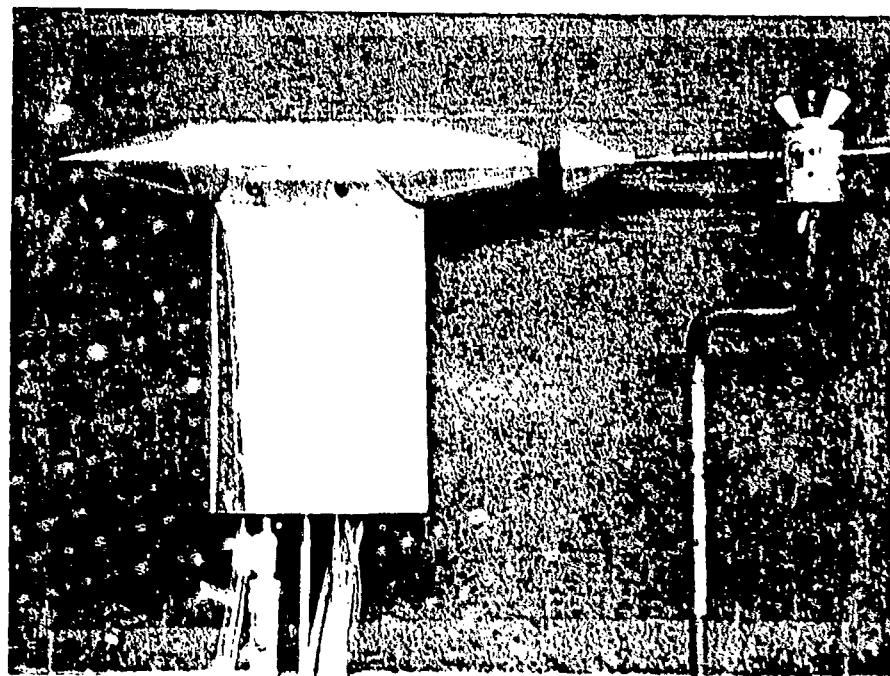


Figure 4b. Model with Fairing over Lines
and Thrust Reverser Mounted

Table 1
Test Condition Matrix

Test Nos.	Thrust Reverser Configuration	Distance reverser mounted aft of nozzle exit (inches)	Nozzle stagnation pressure (psig)	Free-stream velocities* (fps)
1-3	Not installed	-	0	51.3, 58.7, 70.4 ↓
4-6	↓	-	30	
7-9	Installed	0.125	0	
10-12	↓	↓	10	
13-15	↓	↓	15	
16-18	↓	↓	20	
19-21	↓	↓	25	
22-24	↓	↓	30	
25-27	Installed	0.250	0	
28-30	↓	↓	10	
31-33	↓	↓	15	
34-36	↓	↓	20	
37-39	↓	↓	25	
40-42	↓	↓	30	
*Note: Tests were also run at zero free-stream velocity.				

Test Results

Static pressures were measured at four locations on the afterbody and at several forward stations as well. These pressures were converted into pressure coefficients. Plots of pressure coefficient versus body location are presented in Appendix B.

The test data are discussed in Section V.

V. Solution of Flow Equations

Time and funds available did not allow completion of the solution of the equations or a complete interpretation of the test data. However a representative test case for no free stream flow was chosen and programmed for solution on the computer. The input data for this case are summarized in Table 2 below.

Table 2
Flow Input Conditions

Geometry:

Afterbody surface slope, ϕ	15°
Angle between initial jet direction and afterbody, θ	30°
Base radius of afterbody, R_b	0.277 in.
Initial width of jet, w_j	0.0021 in.
Jet setback distance, s	0.175 in.

Flow Conditions:

Jet density, ρ	0.00444 sl/ft ³
Initial jet velocity, u_0	1031 fps
Free stream pressure, p_0	2101 psfa
Jet spread parameter, σ	7.7

The equations were programmed in Fortran IV for solution on the University of Lowell Computer System, using a program called ATTACH.

Appendix A contains a printout of the program statements and output, for one particular case corresponding to experimental data.

A plot of the jet trajectory and spread rate for a wall pressure of $p_1 = 2099$ psfa is shown in Figure 5. These plots are from the

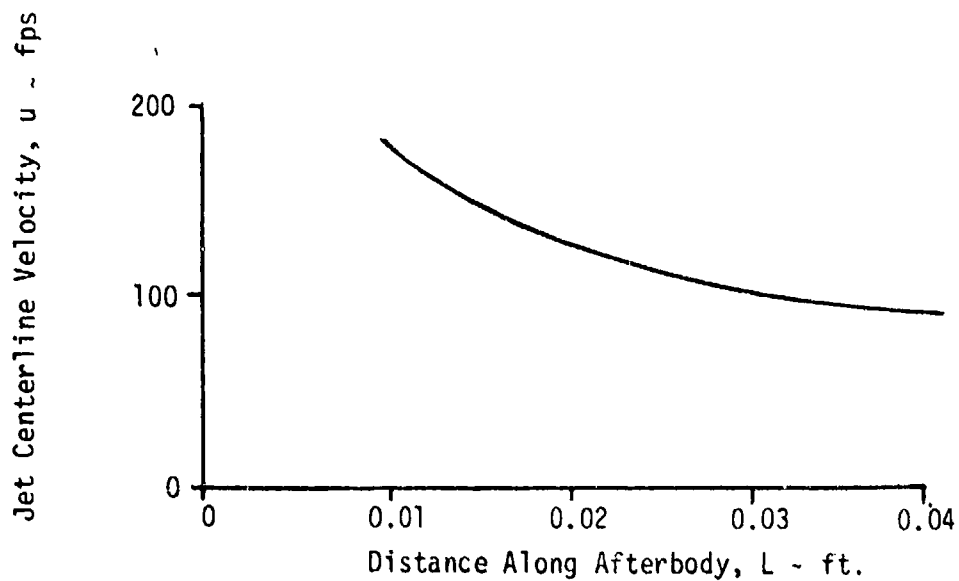


Figure 5a. Variation of Jet Centerline Velocity

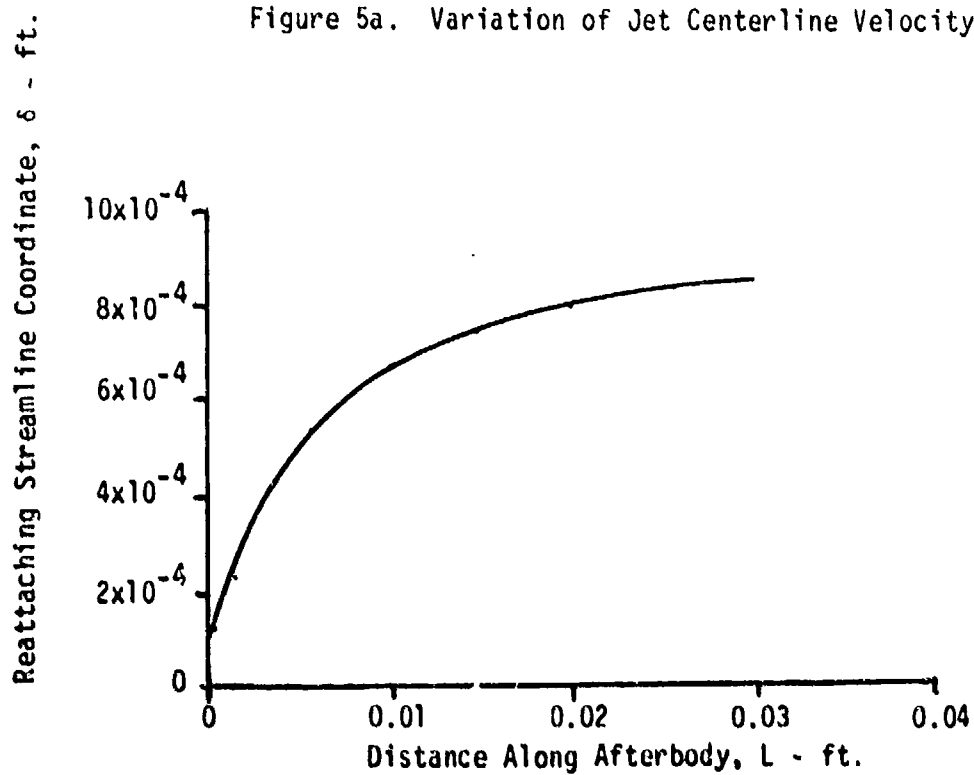


Figure 5b. Jet Spread Variation

computer output of Appendix A. The available time and funds for this research project did not allow the comparison of these calculations with the test data shown in Appendix B.

VI. Recommendations for Future Work

The following recommendations are made for additional work in this area:

- 1) Completion of programming the equations and verification of their validity for certain flow conditions.
- 2) Extension of the development and solution of the equations to the case of an opposing free stream flow.

The following experimental work is needed to verify some of the assumptions used in the theory:

- 3) Flow visualization at low Reynolds numbers by using the existing model in a water channel and photographing the extent of the reversed flow in an opposing free stream. This would be done by using a colored fluid in the exhaust flow to contrast with clear water in the main stream flow.
- 4) Similar visualization of the flow at somewhat higher Reynolds numbers in the low speed wind tunnel using smoke or steam for the exhaust flow and air for the opposing flow.

The experiments described in items 3 and 4 will provide important information on attachment, the extent of reversed flow against the main stream, and verification of the selection of suitable values for the constants K_1 and K_2 and the jet spread equation.

VII. Conclusions

The equations have been derived for the case of attached flow from a thrust reverser impinging on a nozzle-afterbody. These equations were derived for the case of no opposing free stream flow. The portion of these equations for the jet spread and jet trajectory have been programmed in Fortran IV and solved on a computer.

Experiments have been conducted on a small scale model with a target type thrust reverser, and measurements have been made of surface pressure distribution for various combinations of nozzle flow and free stream velocity.

Recommendations have been made for future work. These include additional experiments in flow visualization to aid in determining empirical constants required in the theory, and an extension of the theory to the case of an opposing free-stream flow.

References

1. Tolhurst, W.H., Jr., Kelly, M.W., and Greif, R.K., "Full-Scale Wind Tunnel Investigation of the Effects of a Target-Type Thrust Reverser on the Low-Speed Aerodynamic Characteristics of a Single Engine Jet Airplane," NASA TN D-72, Sept., 1959.
2. Falarski, M.D., and Mort, K.W., "Full-Scale Wind Tunnel Investigation of a Target-Type Thrust Reverser on the A-37B Airplane," NASA TM X-1985, Ames Research Center, April, 1970.
3. Munnicksma, R., "Some Experience with Jet Reverser Model Testing, using Hot and Cold Jets in Ground Proximity," Proc. of the 35th Semi-Annual Meeting of the Supersonic Tunnel Association, Vought Aeronautics Co., Dallas, Texas, March 8-9, 1971.
4. University of Lowell Proposal No.: 82-76, "Reattachment of a Three-Dimensional, Incompressible Jet to an Adjacent Axisymmetric Inclined Surface," University of Lowell Research Foundation, Lowell, MA, 26 October 1981.
5. Bourque, C., and Newman, B.G., "Reattachment of a Two-Dimensional, Incompressible Jet to an Adjacent Flat Plate," The Aeronautical Quarterly, Vol. XI, Aug., 1960.
6. Perry, C.C., "Two-Dimensional Jet Attachment," Ph.D. Dissertation, Mechanical Engineering, University of Michigan, 1967.
7. Olson, R.E., "Reattachment of a Two-Dimensional Compressible Jet to an Adjacent Plate," Presented at the Symposium on Fluid Jet Control Devices, Winter Annual Meeting of ASME, New York, Nov. 28, 1962.
8. Comparin, Glaettli, Mitchell, and Mueller, "On the Limitations and Special Effects in Fluid Jet Amplifiers," Presented at the Symposium on Fluid Jet Control Devices, Winter Annual Meeting of ASME, New York, Nov. 28, 1962.
9. Hoch, J., and Jiji, L.M., "Two-Dimensional Turbulent Offset Jet Boundary Interaction," Journal of Fluids Engineering, Vol. 103, March, 1981.
10. Sarpkaya, T., and Hiriart, G., "Analysis of Curved Target-Type Thrust Reversers," Journal of the American Institute of Aeronautics and Astronautics, Vol. 13, No. 2, February 1975.
11. Whitfield, D.L., "Integral Solution of Compressible Turbulent Boundary Layers Using Improved Velocity Profiles," AEDC-TR-78-42, Arnold Engineering Development Center, Tenn., Dec., 1978.

12. Jacocks, J.L., and Kneile, K.R., "Computation of Three-Dimensional Time-Dependent Flow Using the Euler Equations," AEDC-TR-80-49, Arnold Engineering Development Center, Tenn., July, 1981.
13. Robinson, C.E., "Evaluation of Reynolds Number and Tunnel Wall Porosity Effects on Nozzle Afterbody Drag at Transonic Mach Numbers," AEDC-TR-76-70, July, 1976.

Nomenclature

<u>Symbol</u>	<u>Definition</u>
A	Term expressing area function in control volume
α	Angle to particular location in jet
α'	Value of α at reattachment
A'	Term expressing area function in control volume
C	Surface pressure coefficient, $(p - p_0) / \frac{1}{2} \rho V_0^2$
Δ^D	Distance from surface to jet centerline
Δ'	Value of Δ at reattachment point
δ	Value of y at reattachment streamline border
δ'	Distance from jet center to reattaching streamline
K_1	Fraction of distance in momentum equation
K_2	Fractional portion of pressure difference $(p_s - p_0)$ effective in returning flow
L	Distance along surface of afterbody
L'	Surface distance to point where surface pressure equals jet pressure
p	Local surface pressure
p_e	Pressure external to jet ($p_e = p_0$)
p_i	Pressure inside separation bubble
p_{in}	Nozzle stagnation pressure
ϕ	Afterbody surface slope
p_0	Jet and external pressure
p_s	Stagnation pressure on reattaching streamline
R	Radius of center streamline of jet
R_D	Base radius of afterbody
ρ_0	Density of tunnel flow
ρ_j	Density of jet
R_0	Radius to annular jet from reverser
R_L	Afterbody radius to point where $L = L'$
S	Jet setback distance
σ	Jet spread parameter
θ	Angle between initial jet direction and afterbody surface
u	Velocity at any general position in jet
u_0	Initial jet velocity
v_0	Tunnel test section velocity
w_0	Width or thickness of annular jet
x_L	Distance along curved center streamline
y	Coordinate perpendicular to center streamline
I_0 or J	Initial momentum of jet
I_1	Fraction of forward momentum entrained
I_2	Momentum of return flow from jet
J_2	Momentum of jet at nozzle exit
x_0	Distance measured back to theoretical jet exit, or thrust reverser setback
x'	Value of x at reattachment location

APPENDIX A
Computer Program Printouts

```

      H(1)=01,OUTPUT,TAP=INPUT,TAP=0=OUTPUT)
      WRITE(10,50) X(1),AL(1),RE(1)
      DIMENSION X(50),Y(50),J(1,50),DFLO(3,50),FLW(1,50,50)
      DIMENSION DELT(50)
      REAL L(20)
      PHI = 15.757.295
      TI = 30.757.295
      UJ = 0.00171
      SIG = 7.7
      UU = 1031.
      KMO = .00949
      UJ = .1474
      U = .1455
      X0 = .000355
      PU = 210.
      PI=2099.
      UY= U/PI.
      B = .1231
      AL = .7
      K2 = .7
      L0 = 0
      X10 = 5.28*UJ*UJ+X0*(UU*2.)
      EXFL = .5*UJ*UJ+X0
      WRITE(10,550) EXFL
500 FORMAT(6X,F10.6)
      R = ((KMO*UJ*UJ+X0*2.)/(PU-PI))*2.
      DO 510 I=1,20
      L(I)=L(I-1)+.51
      FLW=0+L(I)*SIN(PHI)
      DEL(I) = R-SQRT((L(I)*COS(TI))^2.+(P-.5*UJ-S-L(I)*SIN(TI))^2.)
      AL(I) = ATAN((L(I)*COS(TI))/(X-L(I)*SIN(TI)-S-.5*UJ))
      DEL(I)' = AL(I)-PHI-TI
      X(I) = EXAL(I)
      XJ = X(I)
400 DO 400 J = 1,50
      Y(J)=Y(J-1)+UY
      Y(1)=0.
      U(I,J) = SQRT((3.+XJ*Y(J))/(4.+KMO*(X(I)+X0)))+(2./EXP(SIG*Y(J))
      /(X(I)+X0))+1./EXP(SIG*Y(J)/(X(I)+X0)))**2.
410 DFLO(I,J) = J(I,J)*(X(L+DEL(I))-Y(J))*COS(DEL(I)).
407 DO 400 J = 1,50
      NUMERICALLY INTEGRATE VELOCITY DISTRIBUTION TO FIND HEAT TRANSFER
      FLG(I,J) = AREA(DFLO,I,J,UY)
      WRITE(10,410) L(I),Y(I),U(I,J),FLW(I,J),DFLO(I,J)
420 FORMAT(5X,F8.4,F10.5,F14.6,F10.5,F15.6)
      IF((FLW(I,J)-EXFL).GT.0.) GO TO 500
430 CONTINUE
500 DELT(I) = Y(J)
      WRITE (10,520) X(I), DELT(I)
510 FORMAT(6X,F8.4,6X,F12.5)
540 IF(DELT(I)-DELT(1)) 5+5,550,55
540 CONTINUE
550 CONTINUE
      END

```

Copy available to DTIC does not
warrant fully legible reproduction

00100	000393	103.122237	002124	0.022119
00100	000420	101.021247	002137	0.071.44
00100	000427	10.003050	002140	0.114440
00100	000430	10.001702	002154	0.0004.1
00100	000439	101.111212	002155	0.021010
00100	000440	10.001249	002157	0.000100
00100	000513	100.271359	002177	0.0711.7
00100	000530	100.061024	002190	0.1430.1
00100	000547	100.021009	002207	0.001200
00100	000564	10.001004	002211	0.001719
00100	000561	147.134010	002213	0.0002.4
00100	000570	140.004004	002214	0.0000.1
00100	000610	144.021000	002214	0.0000.7
00100	000630	143.201003	002214	0.7007.0
00100	000631	14.000034	002214	0.7000.7
00100	000667	139.100070	002214	0.0011.4
00100	000667	139.100070	002214	0.0712.0
00200	000000	104.122224	002214	0.0000.0
00200	000017	104.117408	002214	0.0000.0
00200	000034	104.100001	002214	0.0000.0
00200	000051	104.070007	002214	0.0000.0
00200	000060	104.000000	002214	0.0000.0
00200	000070	104.000000	002214	0.0000.0
00200	000080	104.000000	002214	0.0000.0
00200	000090	104.000000	002214	0.0000.0
00200	000100	104.000000	002214	0.0000.0
00200	000110	104.000000	002214	0.0000.0
00200	000120	104.000000	002214	0.0000.0
00200	000130	104.000000	002214	0.0000.0
00200	000140	104.000000	002214	0.0000.0
00200	000150	104.000000	002214	0.0000.0
00200	000160	104.000000	002214	0.0000.0
00200	000170	104.000000	002214	0.0000.0
00200	000180	104.000000	002214	0.0000.0
00200	000190	104.000000	002214	0.0000.0
00200	000200	104.000000	002214	0.0000.0
00200	000210	104.000000	002214	0.0000.0
00200	000220	104.000000	002214	0.0000.0
00200	000230	104.000000	002214	0.0000.0
00200	000240	104.000000	002214	0.0000.0
00200	000250	104.000000	002214	0.0000.0
00200	000260	104.000000	002214	0.0000.0
00200	000270	104.000000	002214	0.0000.0
00200	000280	104.000000	002214	0.0000.0
00200	000290	104.000000	002214	0.0000.0
00200	000300	104.000000	002214	0.0000.0
00200	000310	104.000000	002214	0.0000.0
00200	000320	104.000000	002214	0.0000.0
00200	000330	104.000000	002214	0.0000.0
00200	000340	104.000000	002214	0.0000.0
00200	000350	104.000000	002214	0.0000.0
00200	000360	104.000000	002214	0.0000.0
00200	000370	104.000000	002214	0.0000.0
00200	000380	104.000000	002214	0.0000.0
00200	000390	104.000000	002214	0.0000.0
00200	000400	104.000000	002214	0.0000.0
00200	000410	104.000000	002214	0.0000.0
00200	000420	104.000000	002214	0.0000.0
00200	000430	104.000000	002214	0.0000.0
00200	000440	104.000000	002214	0.0000.0
00200	000450	104.000000	002214	0.0000.0
00200	000460	104.000000	002214	0.0000.0
00200	000470	104.000000	002214	0.0000.0
00200	000480	104.000000	002214	0.0000.0
00200	000490	104.000000	002214	0.0000.0
00200	000500	104.000000	002214	0.0000.0
00200	000510	104.000000	002214	0.0000.0
00200	000520	104.000000	002214	0.0000.0
00200	000530	104.000000	002214	0.0000.0
00200	000540	104.000000	002214	0.0000.0
00200	000550	104.000000	002214	0.0000.0
00200	000560	104.000000	002214	0.0000.0
00200	000570	104.000000	002214	0.0000.0
00200	000580	104.000000	002214	0.0000.0
00200	000590	104.000000	002214	0.0000.0
00200	000600	104.000000	002214	0.0000.0
00200	000610	104.000000	002214	0.0000.0
00200	000620	104.000000	002214	0.0000.0
00200	000630	104.000000	002214	0.0000.0
00200	000640	104.000000	002214	0.0000.0
00200	000650	104.000000	002214	0.0000.0
00200	000660	104.000000	002214	0.0000.0
00200	000670	104.000000	002214	0.0000.0
00200	000680	104.000000	002214	0.0000.0
00200	000690	104.000000	002214	0.0000.0
00200	000700	104.000000	002214	0.0000.0
00200	000710	104.000000	002214	0.0000.0
00200	000720	104.000000	002214	0.0000.0
00200	000730	104.000000	002214	0.0000.0
00200	000740	104.000000	002214	0.0000.0
00200	000750	104.000000	002214	0.0000.0
00200	000760	104.000000	002214	0.0000.0
00200	000770	104.000000	002214	0.0000.0
00200	000780	104.000000	002214	0.0000.0
00200	000790	104.000000	002214	0.0000.0
00200	000800	104.000000	002214	0.0000.0
00200	000810	104.000000	002214	0.0000.0
00200	000820	104.000000	002214	0.0000.0
00200	000830	104.000000	002214	0.0000.0
00200	000840	104.000000	002214	0.0000.0
00200	000850	104.000000	002214	0.0000.0
00200	000860	104.000000	002214	0.0000.0
00200	000870	104.000000	002214	0.0000.0
00200	000880	104.000000	002214	0.0000.0
00200	000890	104.000000	002214	0.0000.0
00200	000900	104.000000	002214	0.0000.0
00200	000910	104.000000	002214	0.0000.0
00200	000920	104.000000	002214	0.0000.0
00200	000930	104.000000	002214	0.0000.0
00200	000940	104.000000	002214	0.0000.0
00200	000950	104.000000	002214	0.0000.0
00200	000960	104.000000	002214	0.0000.0
00200	000970	104.000000	002214	0.0000.0
00200	000980	104.000000	002214	0.0000.0
00200	000990	104.000000	002214	0.0000.0
00200	001000	104.000000	002214	0.0000.0

Best Available Copy

Copy available to DTIC from 2011
 without fully feasible reproduction

0300	000000	99.721239	0.000000	0.345862
0300	000001	99.719811	0.000001	0.344324
0300	000002	99.714725	0.000002	0.342612
0300	000003	99.705585	0.000003	0.340725
0300	000004	99.692159	0.000004	0.338605
0300	000005	99.675340	0.000005	0.336453
0300	000006	99.655848	0.000006	0.334217
0300	000007	99.634147	0.000007	0.331848
0300	000008	99.611719	0.000008	0.329390
0300	000009	99.589455	0.000009	0.326771
0300	000010	99.568577	0.000010	0.324075
0300	000011	99.549452	0.000011	0.321347
0300	000012	99.532117	0.000012	0.318587
0300	000013	99.516545	0.000013	0.315787
0300	000014	99.502753	0.000014	0.312956
0300	000015	99.490745	0.000015	0.310085
0300	000016	99.480523	0.000016	0.307185
0300	000017	99.472108	0.000017	0.304255
0300	000018	99.465492	0.000018	0.301297
0300	000019	99.460588	0.000019	0.298311
0300	000020	99.457273	0.000020	0.295297
0300	000021	99.455455	0.000021	0.292256
0300	000022	99.455124	0.000022	0.289187
0300	000023	99.457224	0.000023	0.286091
0300	000024	99.461747	0.000024	0.282969
0300	000025	99.468424	0.000025	0.279821
0300	000026	99.477356	0.000026	0.276647
0300	000027	99.488631	0.000027	0.273449
0300	000028	99.502451	0.000028	0.270227
0300	000029	99.518937	0.000029	0.266981
0300	000030	99.537479	0.000030	0.263711
0300	000031	99.557939	0.000031	0.260417
0300	000032	99.580252	0.000032	0.257099
0300	000033	99.604444	0.000033	0.253757
0300	000034	99.630511	0.000034	0.250391
0300	000035	99.658471	0.000035	0.246999
0300	000036	99.688221	0.000036	0.243581
0300	000037	99.719761	0.000037	0.240137
0300	000038	99.753083	0.000038	0.236667
0300	000039	99.788194	0.000039	0.233171
0300	000040	99.825003	0.000040	0.229649
0300	000041	99.863511	0.000041	0.226091
0300	000042	99.902719	0.000042	0.222497
0300	000043	99.942627	0.000043	0.218867
0300	000044	99.983235	0.000044	0.215201
0300	000045	100.024543	0.000045	0.211509
0300	000046	100.066551	0.000046	0.207791
0300	000047	100.109259	0.000047	0.204047
0300	000048	100.152667	0.000048	0.200277
0300	000049	100.196775	0.000049	0.196481
0300	000050	100.241583	0.000050	0.192659
0300	000051	100.287091	0.000051	0.188811
0300	000052	100.333309	0.000052	0.184937
0300	000053	100.380237	0.000053	0.181037
0300	000054	100.427875	0.000054	0.177111
0300	000055	100.476223	0.000055	0.173159
0300	000056	100.525281	0.000056	0.169181
0300	000057	100.575049	0.000057	0.165177
0300	000058	100.625527	0.000058	0.161147
0300	000059	100.676705	0.000059	0.157091
0300	000060	100.728583	0.000060	0.153009
0300	000061	100.781161	0.000061	0.148901
0300	000062	100.834439	0.000062	0.144767
0300	000063	100.888417	0.000063	0.140607
0300	000064	100.943095	0.000064	0.136421
0300	000065	101.000000	0.000065	0.132209
0300	000066	101.058041	0.000066	0.127971
0300	000067	101.117219	0.000067	0.123707
0300	000068	101.177533	0.000068	0.119417
0300	000069	101.238983	0.000069	0.115101
0300	000070	101.301569	0.000070	0.110759
0300	000071	101.365291	0.000071	0.106391
0300	000072	101.430149	0.000072	0.102007
0300	000073	101.496143	0.000073	0.097597
0300	000074	101.563273	0.000074	0.093161
0300	000075	101.631539	0.000075	0.088699
0300	000076	101.700941	0.000076	0.084211
0300	000077	101.771479	0.000077	0.079697
0300	000078	101.843153	0.000078	0.075157
0300	000079	101.915963	0.000079	0.070591
0300	000080	101.989909	0.000080	0.066009
0300	000081	102.064991	0.000081	0.061411
0300	000082	102.141209	0.000082	0.056797
0300	000083	102.218563	0.000083	0.052167
0300	000084	102.297053	0.000084	0.047521
0300	000085	102.376679	0.000085	0.042859
0300	000086	102.457441	0.000086	0.038181
0300	000087	102.539339	0.000087	0.033487
0300	000088	102.622373	0.000088	0.028777
0300	000089	102.706543	0.000089	0.024051
0300	000090	102.791849	0.000090	0.019309
0300	000091	102.878291	0.000091	0.014551
0300	000092	102.965869	0.000092	0.009777
0300	000093	103.054583	0.000093	0.004987
0300	000094	103.144433	0.000094	0.000181
0300	000095	103.235419	0.000095	0.000000
0300	000096	103.327541	0.000096	0.000000
0300	000097	103.420799	0.000097	0.000000
0300	000098	103.515183	0.000098	0.000000
0300	000099	103.610693	0.000099	0.000000

Best-Available Copy

Copy available to DTIC does not
include fully legible reproduction

.0400	.000257	85.196677	.001298	5.044117
.0400	.000274	85.173759	.001334	5.041303
.0400	.000291	85.149393	.001470	5.038623
.0400	.000308	85.123547	.001557	5.035796
.0400	.000325	85.096241	.001643	5.032884
.0400	.000342	85.067459	.001729	5.029886
.0400	.000359	85.037234	.001815	5.026883
.0400	.000376	85.005541	.001901	5.023854
.0400	.000393	84.972332	.001986	5.020801
.0400	.000410	84.937785	.002072	5.017741
.0400	.000427	84.901727	.002158	5.014681
.0400	.000445	84.864218	.002244	5.011629
.0400	.000462	84.825263	.002329	5.008517
.0400	.000479	84.784862	.002415	5.005284
.0400	.000496	84.743020	.002500	4.999901
.0400	.000513	84.699738	.002586	4.995286
.0400	.000530	84.655020	.002671	4.991399
.0400	.000547	84.608859	.002757	4.987249
.0400	.000564	84.561289	.002842	4.983226
.0400	.000581	84.512280	.002927	4.979050
.0400	.000598	84.461849	.003012	4.974772
.0400	.000616	84.409998	.003097	4.970432
.0400	.000633	84.356730	.003182	4.966049
.0400	.000650	84.302050	.003267	4.961566
.0400	.000667	84.245951	.003352	4.956921
.0400	.000684	84.188455	.003437	4.952255
.0400	.000701	84.129571	.003521	4.947549
.0400	.000718	84.069273	.003606	4.942860
.0400	.000735	84.007592	.003690	4.937775
.0400	.000752	83.944517	.003775	4.932789
.0400	.000769	83.880057	.003859	4.927723
.0400	.000787	83.814217	.003943	4.922578
.0400	.000804	83.747021	.004027	4.917354
.0400	.000821	83.678413	.004111	4.912152
.0400	.000838	83.608459	.004195	4.906871
.0444	.000855	83.537199		

Copy available to DTIC does not
 permit fully legible reproduction

APPENDIX B

Summary of Test Data
Pressure Coefficient Plots

WITHOUT THRUST REVERSER

$$P_{th} = 0$$

Distance From Nose, inches

4 5 6 7
7 1/2 8 8 1/2 9 1/2

Pressure Coefficient, C_p

.4
.3
.2
.1
0
.1
.2
.3
.4
.5
.6

$V_{0.07} = 418$
40
35

Separation for 40 & 35

.4
.3
.2
.1
0
-.1
-.2
-.3
-.4
-.5
-.6

0.1

WITHOUT THRUST REVERSER

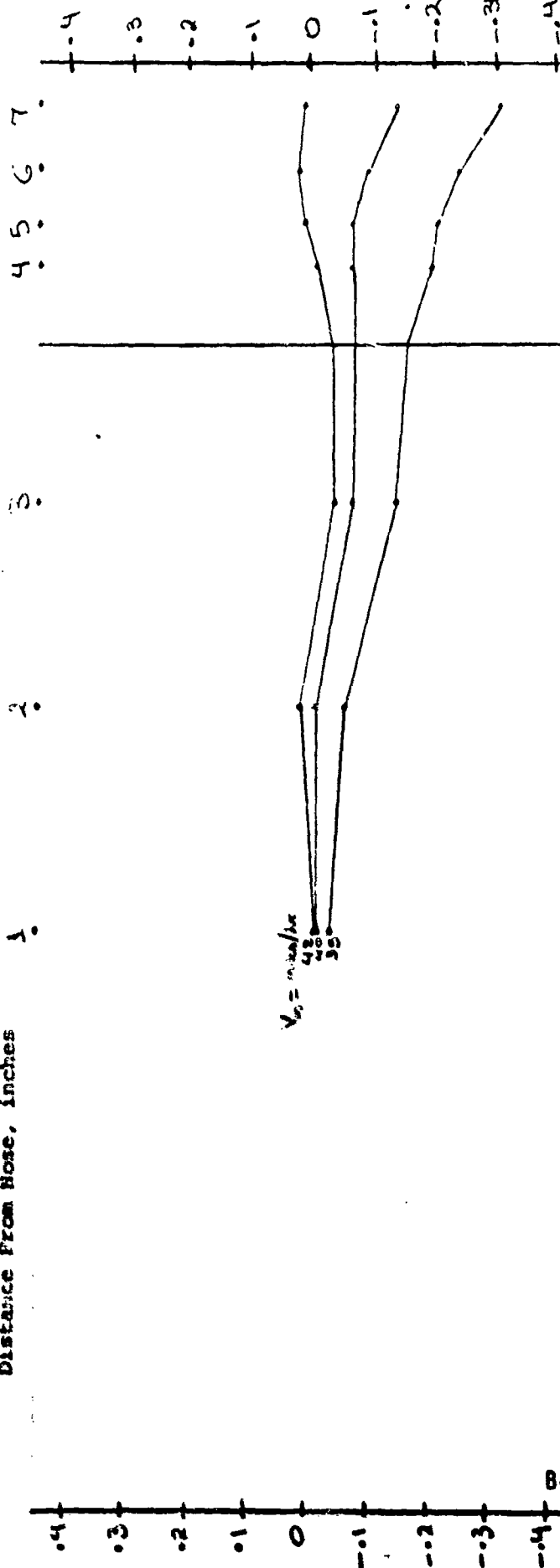
$P_{in} = 30 \text{ psig}$

Distance From Nose, inches

Pressure Coefficient, C_p

$V_{in} = \text{inches/sec}$
48
40
35

B-2



WITH THRUST REVERSER

at $x = +1/8$

$P_{in} = 0$

Distance From Nose, inches

1

2

3

4

5

6

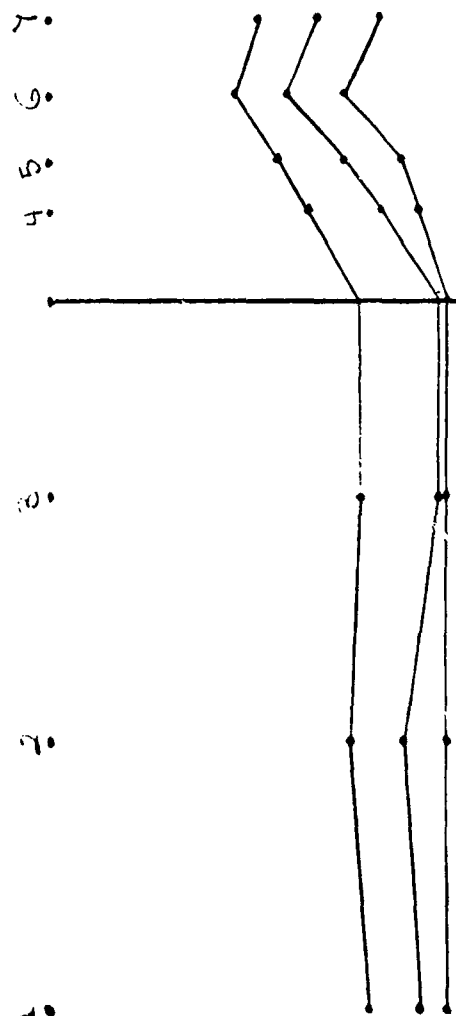
7

Pressure Coefficient, C_p

-.4
-.3
-.2
-.1
0
-.1
-.2
-.3
-.4

-.4
-.3
-.2
-.1
0
-.1
-.2
-.3
-.4

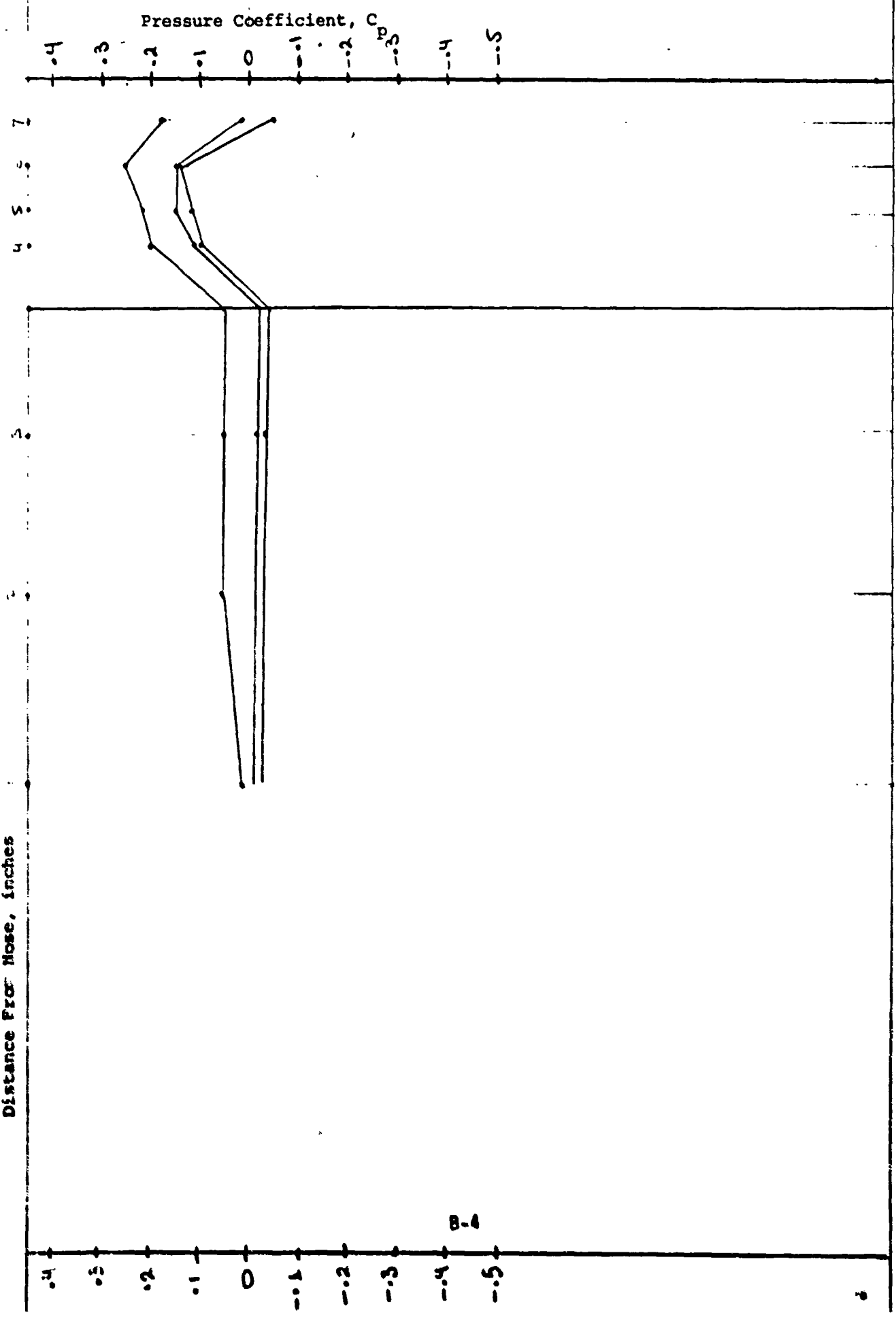
B-3



WITH $x = \frac{1}{8}$
 THRUST REVERSE

$P_{in} = 10 \text{ psig}$

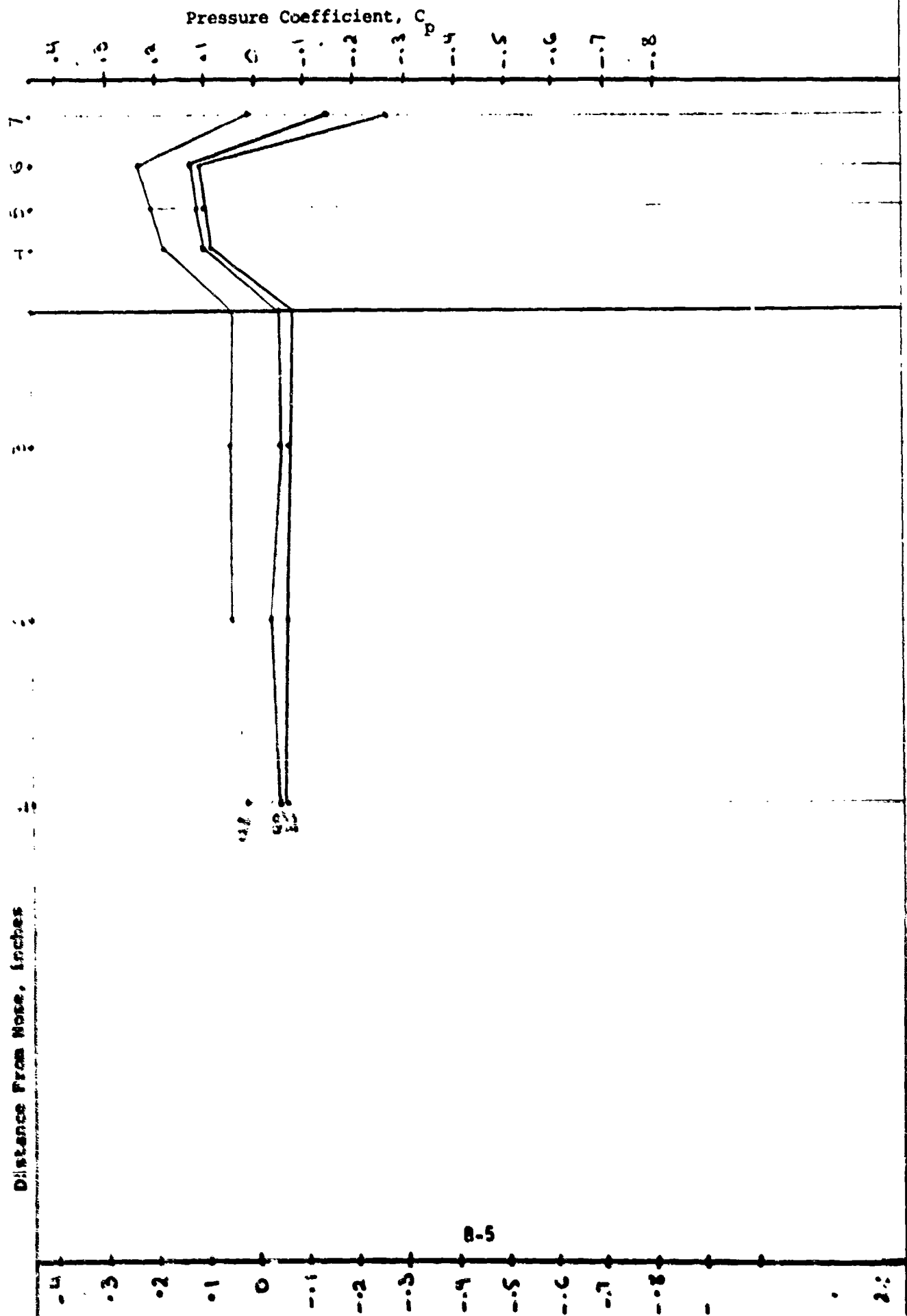
Distance From Nose, inches



B-4

WITH $\alpha = \frac{1}{8}$
THrust REVERSER

$P_{in} = 15 \text{ psig}$

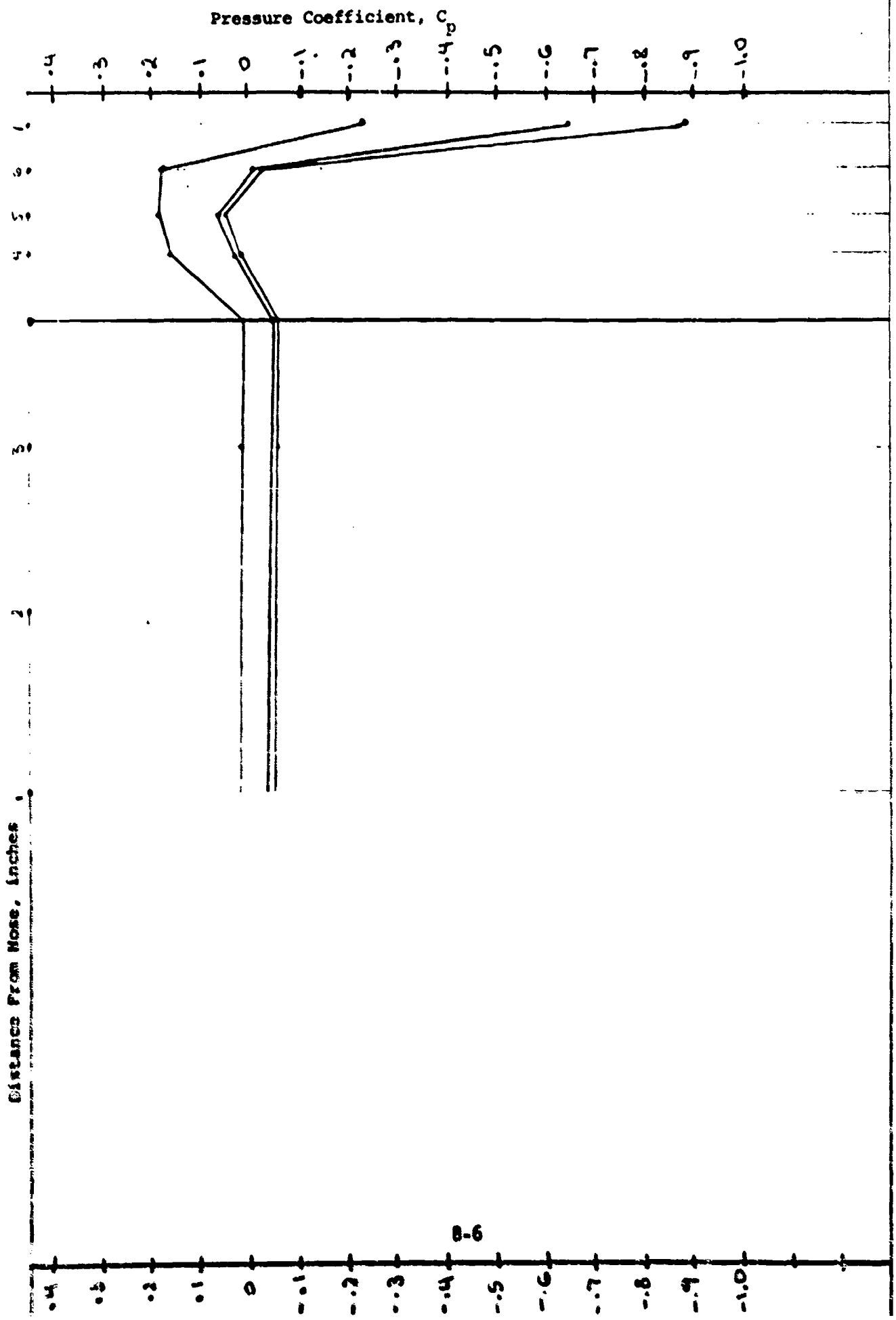


B-5

$R_{ue} = 20 \text{ psig}$

WITH $X = +\frac{1}{8}$
THrust Reverser

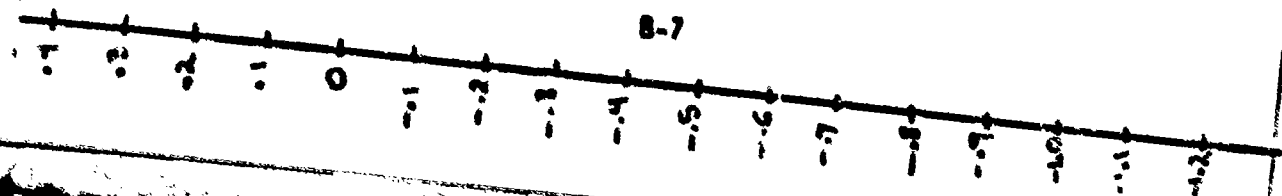
Distance From Nose, inches



WITH $\Delta = +\frac{1}{8}$
THrust REVERSE

Distance From Nose, inches

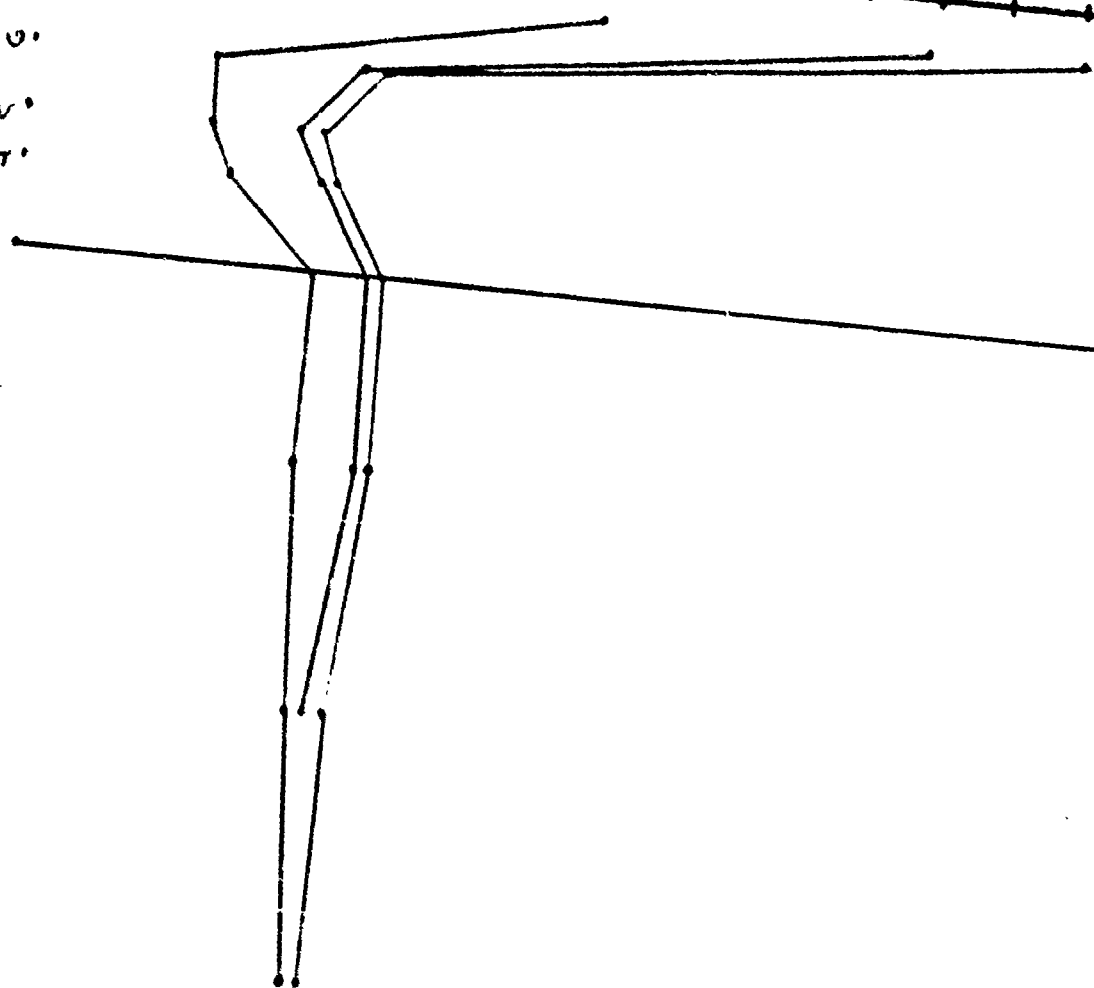
$P_H = 25 \text{ psig}$



1

2

4 5 6 7



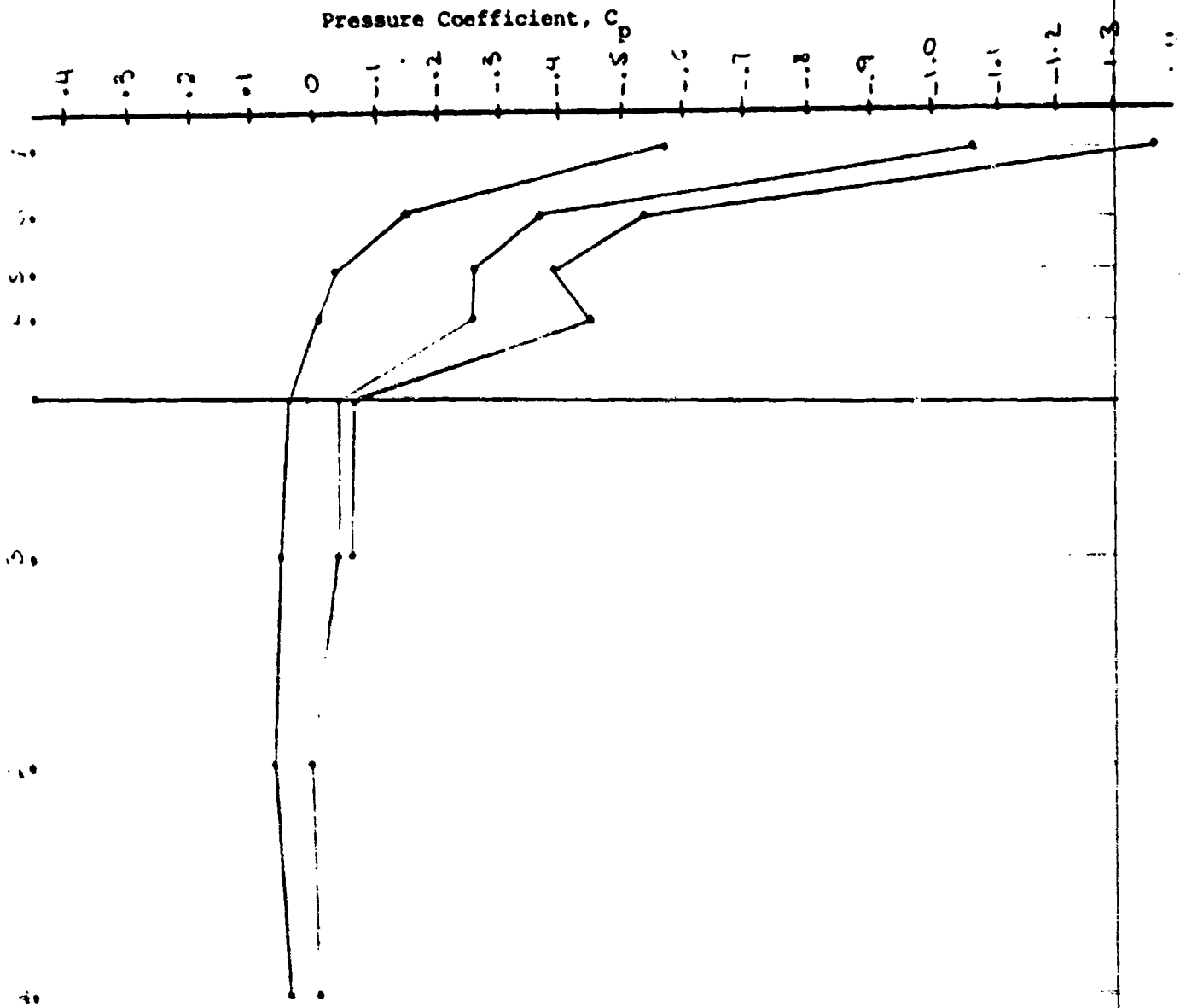
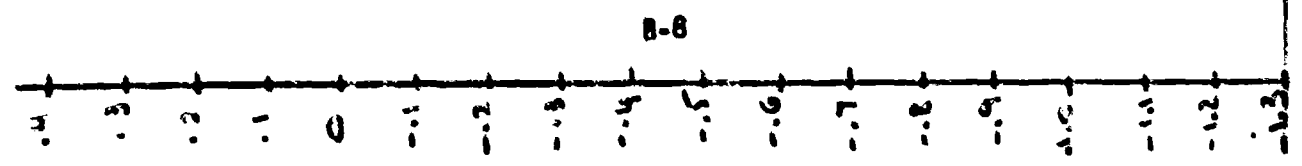
Pressure Coefficient, C_p

$\alpha = 1/8$

$P_n = 30 \text{ psi g}$

THrust REVERSER

Distance From Nose, inches

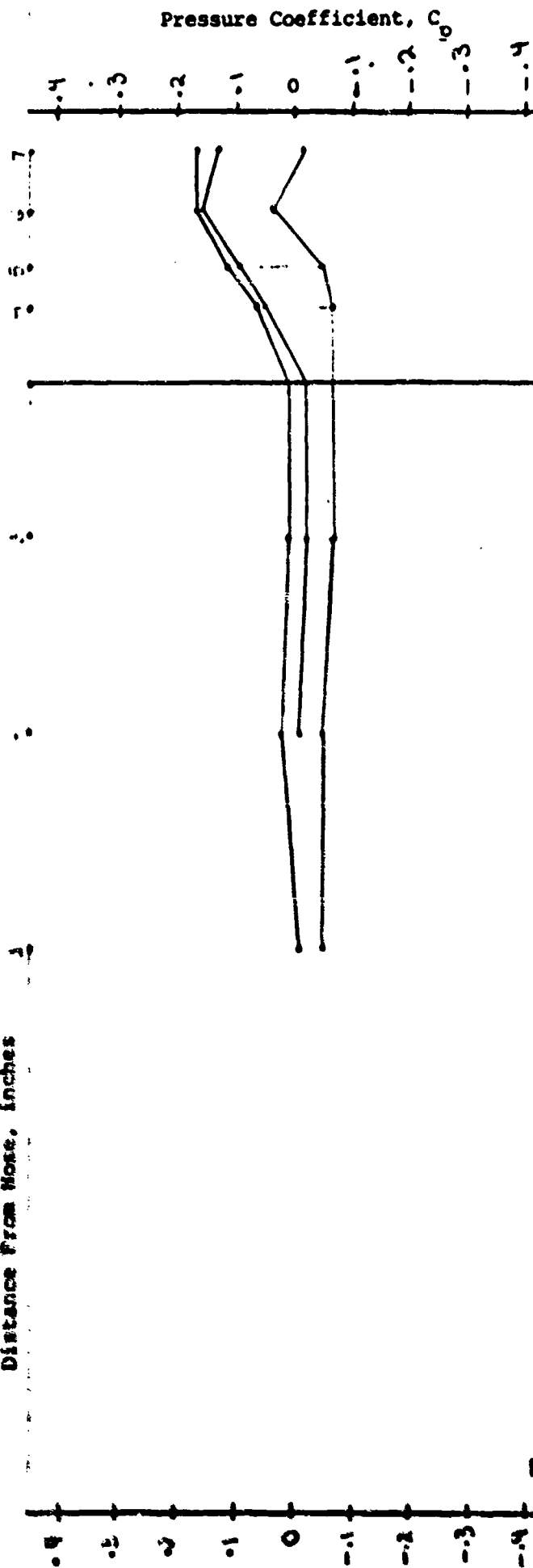


B-8

WITH $\alpha = +1/4$
 THRUST REVERSED

Distance From Nose, inches

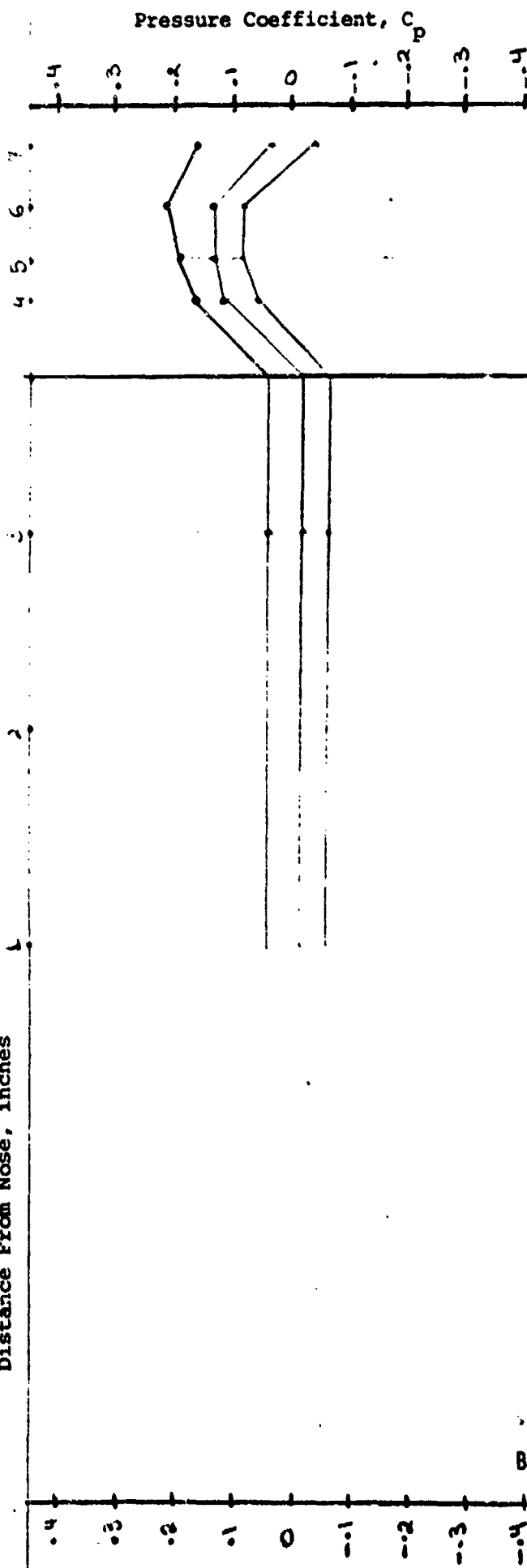
$P_{\infty} = 0$



$P_w = 10 \text{ psi}$

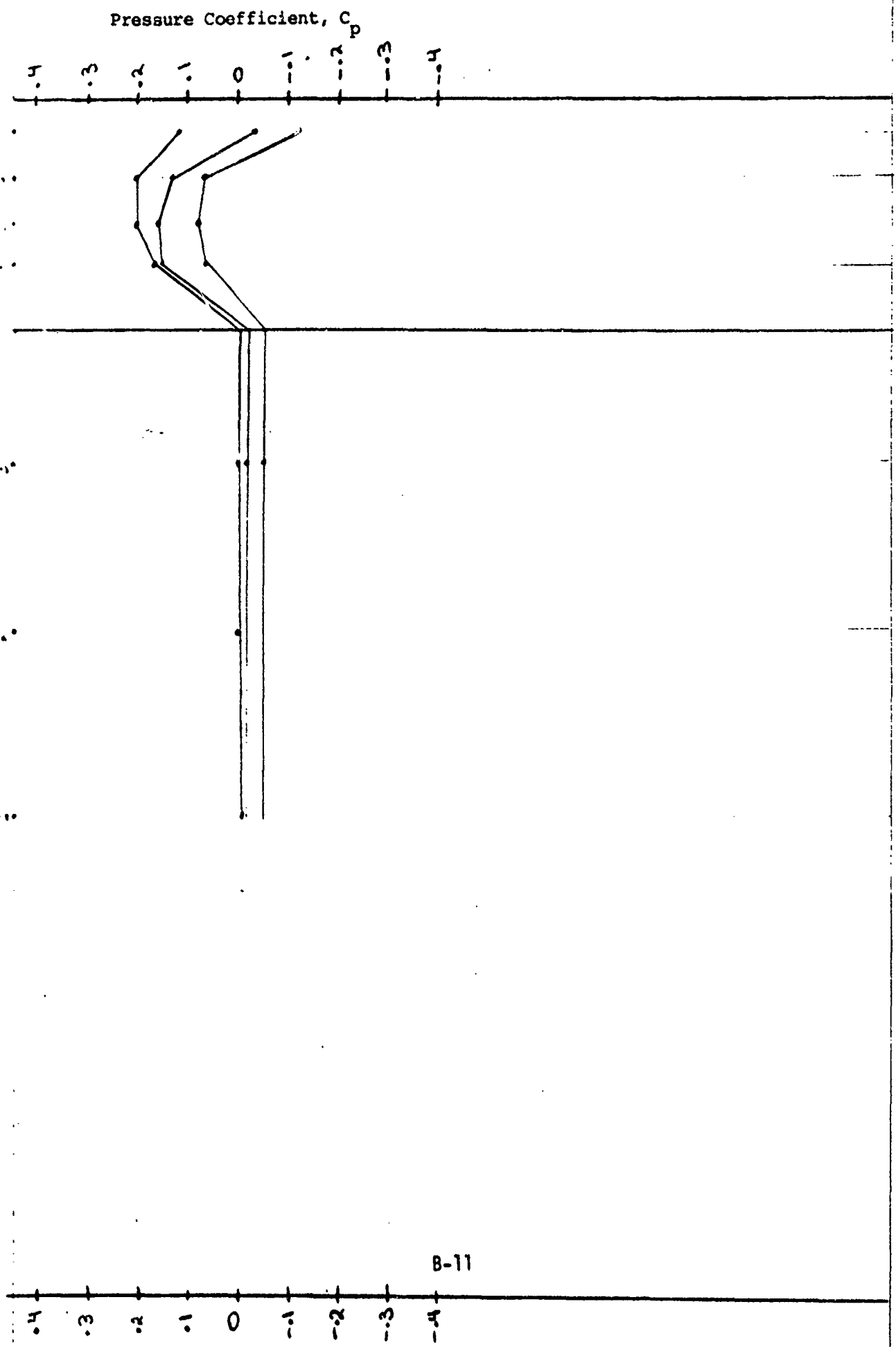
WITH $\chi = +\frac{1}{4}$
THrust Reverser

Distance From Nose, inches



with $\lambda = 1/4$
 Thrust Reverser
 Distance From Nose, inches

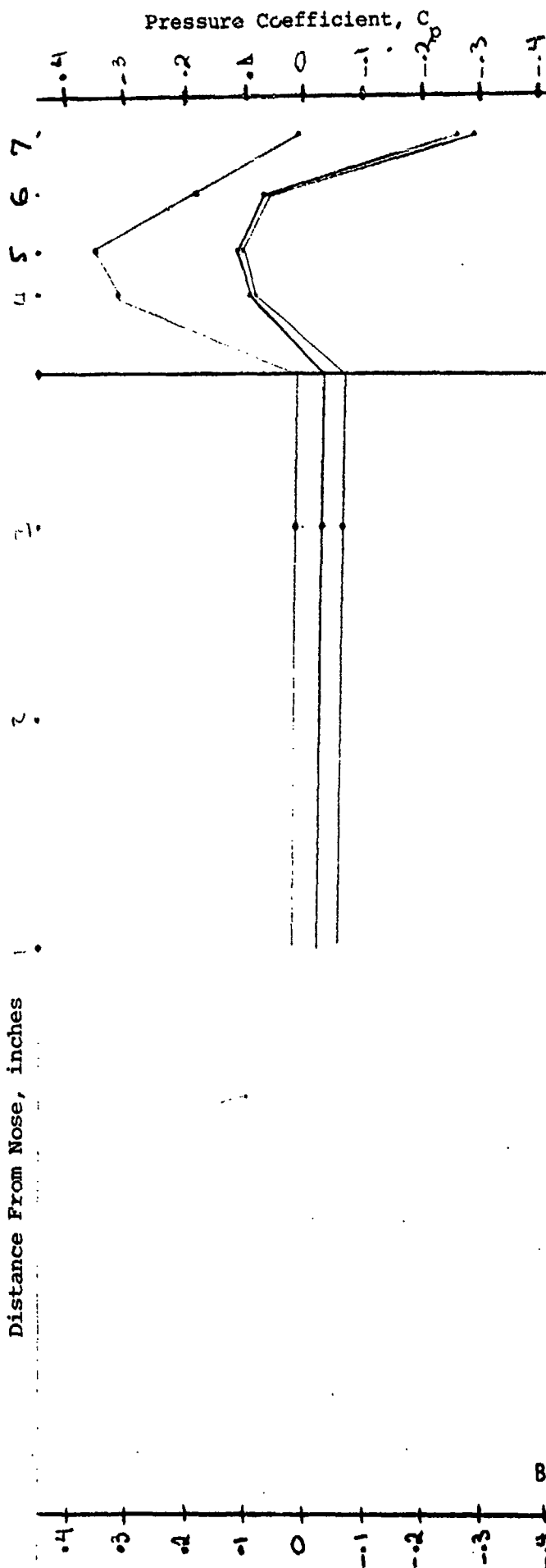
$P_{1W} = 15 \text{ psig}$



WITH $x = \frac{1}{4}$
THrust Forward

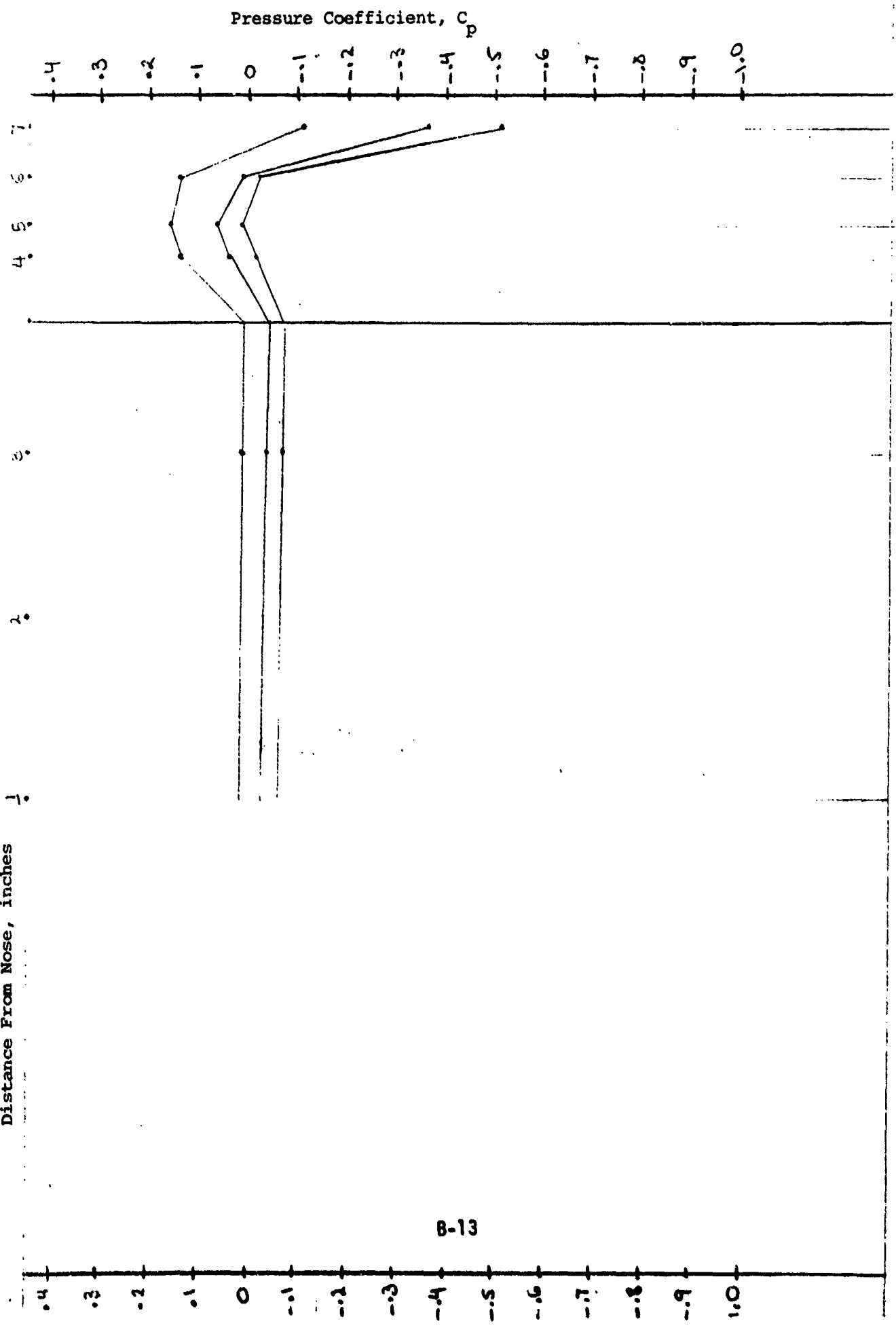
$R_n = 200 \text{ jig}$

Distance From Nose, inches



WITH $\chi = +\frac{1}{4}$
 THRU REVERSE
 Distance From Nose, inches

$P_{10} = 25 \text{ psig}$



WITH $\alpha = +1/4$
 THROUST REVERSED
 Distance From Nose, inches

$P_{\infty} = 30 \text{ psig}$

